Canadian Mineralogist
Vol. 30, pp. 109-119 (1992)

PLATINUM-GROUP MINERALS IN PYROXENITE FROM THE BOSTON CREEK FLOW BASALTIC KOMATIITE, ABITIBI GREENSTONE BELT, ONTARIO

WILLIAM E. STONE
Department of Geology, McMaster University, Hamilton, Ontario L8S 4M1

MICHAEL E. FLEET
Department of Geology, University of Western Ontario, London, Ontario N6A 5B7

JAMES H. CROCKET
Department of Geology, McMaster University, Hamilton, Ontario L8S 4M1

DAVID M. KINGSTON
Department of Geology, University of Western Ontario, London, Ontario N6A 5B7

ABSTRACT

The first occurrence of platinum-group minerals (PGM) in Abitibi belt volcanic rocks has been discovered in pyroxenite from the Boston Creek Flow basaltic komatiite, Ontario. The PGM observed are bismuthian merenskyite, merenskyite, bismuthian kotulskite, mertieite or stibiopalladinite, an unnamed Pd–Ag sulfide, sperrylite, and an unnamed Rh–Pt sulfarsenide. The grains are submicrometric to 15 μm in diameter, making *in situ* analysis difficult. The mineralization was observed in samples of clinopyroxenite and spinel (Fe–Ti oxide) clinopyroxenite collected at the margins of a 7-m-thick zone of altered pyroxenite. The platinum mineralization is characterized by spatial association with Cu–Fe sulfides, native gold, electrum, and a suite of silver minerals, and with secondary silicate alteration of Fe–Ti oxide and groundmass. There is an absence of nickel sulfide. Textural evidence and spatial associations indicate that the mineralization originated by hydrothermal processes. Hydrothermal fluid activity accompanying cooling of the flow or later greenschist-facies metamorphism appears to have mobilized and reconcentrated PGE during alteration of Fe–Ti oxide and brittle deformation.

Keywords: platinum-group minerals, merenskyite, kotulskite, sperrylite, gold, naumannite, hessite, Boston Creek Flow, basaltic komatiite, analytical data, Abitibi belt, Ontario.

SOMMAIRE

Nous décrivons le premier exemple de minéraux du groupe du platine dans la ceinture de roches vertes de l'Abitibi, dans une pyroxénite provenant de la coulée de komatiite basaltique dite de Boston Creek, en Ontario. Parmi ces minéraux se trouvent merenskyite bismuthifère, merenskyite, kotulskite bismuthifère, mertieite ou stibiopalladinite, un sulfure à Pd–Ag sans nom, sperrylite, et un sulfarséniure à Rh–Pt sans nom. Les grains sont submicrométriques, et atteignent 15 μm de diamètre, ce qui rend leur analyse *in situ* difficile. Ce sont des échantillons de clinopyroxénite et de clinopyroxénite à spinelle (oxyde Fe–Ti) à la marge d'une zone altérée de 7 m qui contiennent ces minéraux. La minéralisation montre une association dans l'espace avec sulfures de Cu–Fe, or natif, électrum, et une suite de minéraux argentifères, et avec des silicates secondaires qui remplacent l'oxyde à Fe–Ti et la pâte. Le sulfure de Ni est absent. D'après les textures et ces associations dans l'espace, la minéralisation résulterait d'un phénomène hydrothermal. L'activité d'une phase fluide au cours du refroidissement de la coulée ou d'un épisode de métamorphisme ultérieur dans le facies schistes verts aurait mobilisé et concentré les éléments du groupe du platine pendant l'altération de l'oxyde à Fe–Ti et la déformation cassante des roches hôtes.

(Traduit par la Rédaction)

Mots-clés: minéraux du groupe du platine, merenskyite, kotulskite, sperrylite, or, naumannite, hessite, coulée de Boston Creek, komatiite basaltique, données analytiques, ceinture de l'Abitibi, Ontario.

INTRODUCTION

The potential of komatiitic rocks for economic platinum-group element (PGE) mineralization is of interest to explorationists and petrologists. In Western Australia, platinum-group minerals (PGM) have been reported in komatiitic host rocks of the Kambalda nickel–copper sulfide deposits (Hudson 1986). PGM also have been reported in the komatiite-hosted O'Toole nickel deposit, Brazil

(Marchetto 1990, Brenner 1990). However, PGM have not been reported in komatiitic and tholeiitic host rocks of the nickel-copper sulfide deposits in the Abitibi greenstone belt, although high contents of PGE have been reported in these rocks (Barnes & Naldrett 1987, Brügmann *et al.* 1987). Knowledge of the mineral host of the PGE in komatiitic rocks is essential to a full understanding of the processes important in concentrating the PGE in these rocks and will lead to refinement of exploration criteria useful in the search for komatiite-hosted PGE deposits in general.

This paper reports the discovery of PGM in pyroxenite from the Boston Creek Flow (BCF) Fe-rich basaltic komatiite (Stone *et al.* 1987), Abitibi greenstone belt, Ontario. The PGM observed are merenskyite, kotulskite, stibiopalladinite or mertieite, Pd–Ag sulfide, sperrylite, and Rh–Pt sulfarsenide. The PGM grains are submicrometric to 15 μm in diameter. They occur in spatial association with Cu–Fe sulfide, native gold, electrum, and a suite of silver minerals, and with secondary silicate alteration of Fe–Ti oxide and groundmass. There is a virtual absence of Ni sulfide. The PGM grains and their spatial associations are described, and processes of possible importance in their origin are discussed. We believe this to be the first published report of PGM in volcanic rocks from the Abitibi belt and in komatiitic volcanic rocks that apparently lack economic Ni–Cu sulfide mineralization.

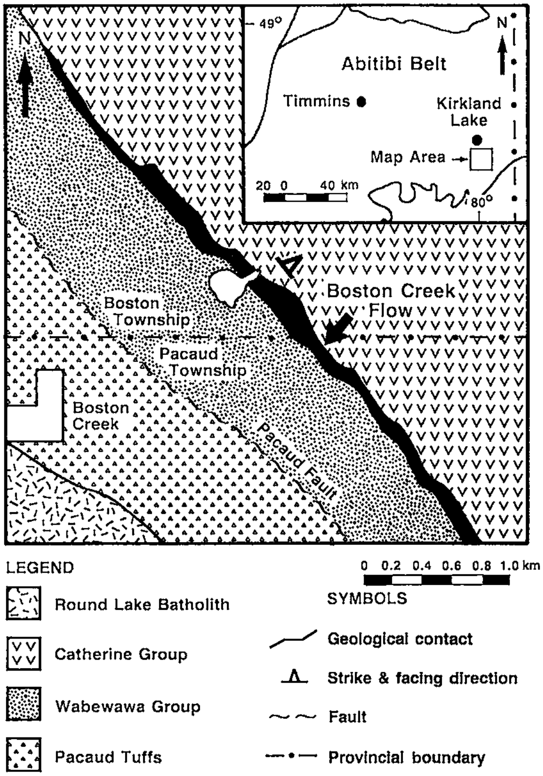

FIG. 1. Location of the Boston Creek Flow.

GEOLOGICAL SETTING

The BCF is a thick, layered iron-rich basaltic komatiite, located in the southern part of the Abitibi greenstone belt, Ontario (Stone *et al.* 1987; Fig. 1). The geology in this part of the belt has been described by Jensen (1985), Corfu *et al.* (1989) and Jackson & Harrap (1989).

The petrography and geochemistry of the BCF have been described by Stone *et al.* (1987). The flow is thick (up to 115 m), layered, and may extend for more than 5 km along strike (Jackson & Harrap 1989). It has up to five layers, which from base to top are: 1) basal pyroxenite, 2) peridotite, 3) pyroxenite, 4) spinel pyroxenite, and 5) spinifex-textured pyroxenite. Previously, the spinel pyroxenite was considered to be gabbro (Stone *et al.* 1987), but a more recent study indicates that the rock is best characterized as spinel pyroxenite (>5 modal % primary Fe–Ti oxide). The BCF is enriched in Fe and depleted in Al compared to other komatiitic and tholeiitic rocks of similar Mg content in the Abitibi belt. Despite recrystallization to greenschist-facies metamorphic minerals (Jolly 1980), primary clinopyroxene and Fe–Ti oxide and igneous textures in the BCF are normally well preserved.

MINERALOGY

The character, distribution, and associations of the PGM grains observed in the BCF are summarized in Table 1 and Figure 2. PGM have been observed in two pyroxenite samples from the flow. One of the samples is from the pyroxenite layer, about 1 m above the contact with the peridotite layer (Fig. 2). The second mineralized sample was collected 7 m farther up-section from the spinel pyroxenite layer, adjacent to the contact with the underlying pyroxenite layer. The two occurrences of mineralization are hereafter referred to as the lower mineralization (LM) and the upper mineralization (UM), respectively. The LM and UM are separated in the flow by 7 m of altered pyroxenite (Fig. 2).

The PGM observed are mainly Pd and Pt minerals. Palladium is present as merenskyite,

TABLE 1. PLATINUM-GROUP MINERALS IN THE BOSTON CREEK FLOW

Mineral	No. of grains LM*	No. of grains UM*	Size	Host
Merenskyite		5	1 to 15 µm	pyrite chalcopyrite amphibole
Kotulskite		>10	1 to 10 µm	chalcopyrite pyrite amphibole
Stibiopalladinite or mertieite	1		<1 µm	amphibole
Pd-Ag sulfide	1		<1 µm	rock fracture
Sperrylite	1	>50	<1 µm	chalcopyrite pyrite kotulskite titanite epidote
Rh-Pt sulfarsenide		1	<1 µm	epidote

* LM, lower mineralization
* UM, upper mineralization

kotulskite, Pd antimonide and Pd–Ag sulfide. Platinum is present mainly as sperrylite. One grain of Rh–Pt sulfarsenide was observed.

Analytical methods

The PGM were discovered, studied and analyzed with a JEOL JXA–8600 microprobe equipped with a Tracor Northern energy-dispersion spectrometer at the University of Western Ontario. The PGM were discovered during detailed electron-microprobe study of samples from the pyroxenite layers. The pyroxenites were chosen for study because an association of Pd and Pt minerals with pyroxenite is known in layered intrusions, such as the Bushveld Complex in South Africa (Mostert *et al.* 1982, Kingston & El-Dosuky 1982), the Great Dyke in Zimbabwe (Wilson & Tredoux 1990), the Penikat complex in Finland (Alapieti & Lahtinen 1986), the Ivrea–Verbano basic complex in Italy (Garuti & Rinaldi 1986), and the Owendale complex in Australia (Johan *et al.* 1989).

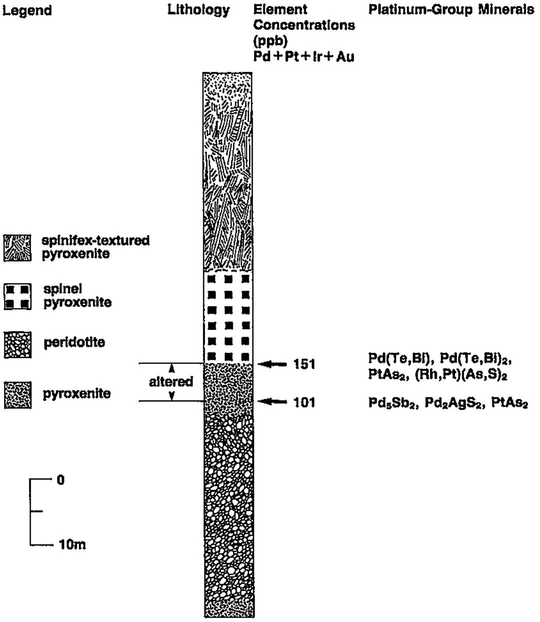

FIG. 2. Schematic section through the Boston Creek Flow showing locations, bulk Σ(Pd + Pt + Ir + Au) values (ppb), and the PGM found in the two mineralized occurrences.

The accuracy of the analyses of PGM grains from the Boston Creek Flow was limited by the ultrafine grain-size. It was not possible to avoid interference caused by beam overlap onto adjacent phases, but techniques were developed to both minimize this interference and to compensate for it. Analyses were made using both wavelength-dispersion techniques (WDS) and energy-dispersion techniques (EDS). WDS analyses were made using an accelerating voltage of 20 kV for a counting time of 20 s, a beam diameter of 2 μm and a beam current of 5 nA. The following peaks were used in the analyses: Fe$K\alpha$, S$K\alpha$, Cu$K\alpha$, Pt$L\alpha$, Pd$L\beta$, As$L\alpha$, Sb$L\alpha$, Ag$L\alpha$, Ni$K\alpha$, Co$K\alpha$, Au$L\alpha$, Te$L\alpha$, Se$L\alpha$, and Bi$L\alpha$. Synthetic FeS and NiS, chalcopyrite and pure metals were used as standards. Ruthenium, Os, and Ir were sought, but not detected (minimum detection limits, in wt.%, were: Ru 0.05, Os 0.11, Ir 0.12). Corrections were made on-line using the ZAF program provided by Tracor Northern, and an additional correction was made for minor interference of Bi and Pt.

EDS analyses of the platinum-group minerals were made at 15 kV for 30 s, with a beam diameter of 1 μm and a Faraday cup current of 2 nA. The EDS technique was used because under WDS conditions (20 kV, 5 nA), the electron beam is much larger (2 μm) than the grains of PGM (*e.g.*, Corrivaux & Laflamme 1990). The same peaks were used as for the WDS analyses, and Rh$L\alpha$ and Bi$M\alpha$ were added. It was necessary to analyze for elements present in the material surrounding the grains of PGM (*e.g.*, Ca$K\alpha$, Mg$K\alpha$, Si$K\alpha$, Ti$K\alpha$, Al$K\alpha$), in order to minimize spectral interferences caused by beam overlap. The same standards were used as for the WDS analyses. Corrections were made on-line using Tracor–Northern's ZAF procedure. Replicate EDS analyses of arsenopyrite, chalcopyrite, FeS, NiS, CdSe, and pure metal standards indicate an accuracy relative to absolute element concentrations of better 3 wt.% for most elements, but only within 8 wt.% for Se.

Low totals obtained for WDS analyses reflect the very small size of the grains analyzed (Tables 2, 3). Fe in the WDS analyses and Fe, Ca, Mg, Si and Al in the EDS analyses normally reflect interference of the surrounding amphibole or sulfide caused by beam overlap during analysis. Attempts were made to correct the analytical data for the effects of interference by subtracting the proportion of Fe, Cu, S, Ca, Mg, Si and Al present in the surrounding material and normalizing to 100% (*e.g.*, Augé 1988). The recalculated compositions in most cases approximate nominal stoichiometries, which appears to validate the correction procedures (*e.g.*, Stone & Fleet 1990).

Further validation of the compositions of the submicrometric blebs comes from comparison of recalculated results of WDS and EDS analyses of a submicrometric bleb of chalcopyrite. The WDS analysis recalculated to 31.53 wt.% Fe, 32.43% S, 35.84% Cu and 0.21% As. The EDS analysis recalculated to 29.8% Fe, 34.6% S and 35.6% Cu. The standard deviation for the averaged compositions of the mineral grains given in Tables 2 and 4 is a maximum of 2.4 wt.% for elements present in amounts in excess of 20 wt.%, 1.2 wt.% for elements present in the range of 5 to 20 wt.%, 0.6 wt.% for elements present in the range of 1 to 5

TABLE 2. AVERAGE COMPOSITION OF PGM GRAINS

Grain	1	2	3	4	5	6	7
Size (µm)	5 x 15	2 x 2	4 x 6	1 x 1	1 x 0.5	1 x 1	1 x 1
Analysis	WDS	EDS	WDS	EDS	EDS	EDS	EDS
n	4	3	4	2	4	3	3
				Raw Data (wt. %)			
Pd	26.48	32.2	40.11	56.1	33.0	2.4	n.d.
Pt	1.04	n.d.	n.d.	n.d.	n.d.	30.8	11.9
Rh	-	-	-	-	-	-	22.3
Ag	n.d.	n.d.	n.d.	n.d.	16.6	n.d.	-
Au	n.d.	n.d.	n.d.	-	-	n.d.	n.d.
Fe	1.50	1.1	1.55	4.1	11.6	4.4	4.9
Ni	-	n.d.	-	n.d.	n.d.	n.d.	n.d.
Cu	0.02	n.d.	n.d.	1.1	1.7	n.d.	n.d.
Ca	-	n.d.	-	3.1	7.2	13.2	7.4
Mg	-	n.d.	-	0.8	3.2	n.d.	n.d.
Si	-	1.1	-	8.3	16.3	7.7	6.3
Al	-	n.d.	-	-	-	n.d.	4.5
Ti	-	-	-	-	-	14.5	0.5
S	0.15	0.6	0.20	n.d.	10.6	n.d.	11.9
Se	n.d.	n.d.	n.d.	-	-	n.d.	n.d.
As	n.d.	n.d.	n.d.	n.d.	n.d.	27.7	29.7
Sb	n.d.	n.d.	0.56	22.6	n.d.	n.d.	n.d.
Te	59.14	63.7	41.82	n.d.	n.d.	n.d.	n.d.
Bi	11.19	n.d.	13.68	-	-	n.d.	n.d.
Total	99.61	98.7	98.00	96.1	100.2	100.7	99.4
				Recalculated (wt. %)			
Pd		33.4		67.0	52.9	4.0	
Pt						50.6	15.3
Rh							28.5
Ag					27.0		
Fe							0.8
Cu				1.3	2.7		
S		0.6			17.5		13.8
As				5.0		45.5	41.6
Sb				26.7			
Te		66.0					
				Recalculated (at. %)			
Pd	31.05	36.9	46.62	67.3	37.2	4.1	
Pt	0.52					28.7	
Rh							20.5
Ag					18.8		
Fe	3.33		3.42				1.0
Cu				2.1	3.2		
S	0.58	2.2	0.76		40.9		31.8
Se							
As				7.2		67.2	41.0
Sb			0.56	23.4			
Te	57.84	60.9	40.53				
Bi	6.67		8.10				

Grain: 1, merenskyite in pyrite; 2, merenskyite in amphibole within altered groundmass; 3, kotulskite in pyrite; 4, stibiopalladinite or mertieite in amphibole within altered groundmass; 6, Pd-Ag sulfide in rock fracture; 6, sperrylite in titanite and amphibole within altered oxide; 7, Rh-Pt sulfarsenide in epidote.
n = number of electron microprobe analyses
- = not determined.
n.d. = not detected; minimum detection limits in wt. % for WDS analyses were: Pt 0.13; Ag 0.14; Au 0.49; Cu 0.14; Se 0.18; As 0.07; Sb 0.20. For EDS analyses, elements with counting statistics <3 X standard deviation were not detected.

TABLE 3. COMPOSITION OF MINERALIZED HOST ROCKS

	LM	UM
SiO_2 (wt.%)	47.32	43.50
TiO_2	1.07	1.98
Al_2O_3	6.21	8.41
Fe_2O_3	16.33	24.65
MnO	0.25	0.25
MgO	11.64	6.72
CaO	14.04	11.97
Na_2O	0.47	1.56
K_2O	0.36	0.35
P_2O_5	0.05	0.08
LOI	2.05	0.29
Total	99.79	99.76
Cu (ppm)	149.5	572.8
Ni	251.4	136.6
S	400.0	600.0
Au (ppb)	48.3	10.4
Ir	0.7	1.6
Pd	32.1	81.2
Pt*	20	58.0

Wt.% and ppm values determined by XRF at McMaster University,
ppb values determined by RNAA with the McMaster Nuclear Reactor.
* Pt value semi-quantitative: see text.

TABLE 4. REPRESENTATIVE COMPOSITIONS OF GRAINS OF ELECTRUM AND SILVER MINERALS

Grain	1	2	3	4	5
Size (µm)	3 x 5	2 x 3	5 x 5	3 x 3	2 x 2
Analysis	EDS	WDS	WDS	EDS	EDS
			Raw Data (wt. %)		
Pd	n.d.	-	n.d.	n.d.	n.d.
Pt	n.d.	-	n.d.	n.d.	n.d.
Ag	31.15	57.89	23.76	66.40	57.38
Au	65.96	-	n.d.	n.d.	31.58
Fe	0.76	5.32	6.97	0.65	1.14
Cu	1.04	4.72	4.90	n.d.	1.62
Ni	n.d.	-	-	n.d.	n.d.
Ca	n.d.	-	-	n.d.	2.09
Mg	n.d.	-	-	n.d.	n.d.
Si	0.41	-	-	0.61	2.03
Al	n.d.	-	-	0.89	0.29
S	n.d.	6.55	8.03	0.20	1.24
Se	n.d.	22.02	24.61	4.57	n.d.
As	n.d.	0.06	n.d.	n.d.	n.d.
Sb	n.d.	n.d.	n.d.	n.d.	n.d.
Te	0.62	0.74	0.36	26.87	2.63
Bi	-	-	25.67	-	-
Total	99.94	97.30	94.30	100.19	99.97
			Recalculated (wt. %)		
Ag	31.06	71.23	31.94	67.59	62.65
Au	68.94				34.48
S		0.76			
Se		27.09	33.07	5.63	
Te		0.91	0.48	26.78	2.87
Bi			34.31		
			Recalculated (at. %)		
Ag	45.49	63.84	33.50	69.03	74.59
Au	54.51				22.59
S		2.30			
Se		33.17	47.39	7.85	
Te		0.69	0.43	23.12	2.82
Bi			18.68		

Grain: 1, electrum in hessite; 2, naumannite in chalcopyrite; 3, Ag-Bi selenide in chalcopyrite in contact with amphibole; 4, hessite in amphibole within altered oxide; 5, aurian silver in hessite.
- = not determined.
n.d. = not detected; minimum detection limits in wt. % for WDS analyses were: Pd 0.16; Pt 0.42; Au 0.49; As 0.13; Sb 0.20. For EDS analyses, elements with counting statistics <3 X standard deviation were not detected.

wt.%, and 0.1 wt.% for elements present in amounts of less than 1 wt.%.

PLATINUM-GROUP MINERALS

Merenskyite

Five grains of merenskyite were observed, all in the UM. One grain is located in a large grain of pyrite within altered Fe–Ti oxide (Fig. 3A). This merenskyite grain, intimately associated with a network of fractures, is in close proximity to a fracture-hosted and multifaceted grain of chalcopyrite (Fig. 3B).

The four other observed grains of merenskyite are present in the altered groundmass, approximately 1 μm in diameter, and bleb-like in shape. Two of them are in the margins of chalcopyrite grains at contact with amphibole; one is in the margin of a composite chalcopyrite–pyrite grain at contact with epidote, in close proximity to a dispersion of sperrylite grains; and one is isolated in the margin of an amphibole grain (Fig. 3C). The composition of the sulfide-associated grains of merenskyite is bismuthian (4.8 to 6.7 at.% Bi; Table 2, grain 1), whereas that of the amphibole-hosted merenskyite lacks Bi (Table 2, grain 2).

Kotulskite

More than ten grains of kotulskite have been observed, but only in the UM. Most of the grains observed are in chalcopyrite and pyrite, 10 μm in maximum dimension, and multifaceted (Figs. 3D, E). One observed grain of kotulskite is submicrometric, bleb-like, and isolated in secondary silicate alteration within the margin of a grains of altered Fe–Ti oxide (Fig. 4B). Kotulskite also occurs as a rim on a core of sperrylite (described below).

Compositions of the kotulskite grains are bismuthian (5.9 to 10.1 at.% Bi). Microprobe analyses indicate the presence of minor amounts of Fe, S, and Sb (*e.g.*, Table 2, grain 3).

Stibiopalladinite or mertieite

The single grain of Pd antimonide observed occurs in the LM, within 50 μm of a grain of Pd–Ag sulfide in amphibolitized groundmass, near large grains and small bleb-like grains of chalcopyrite (Fig. 3F). The Pd antimonide is ovoid and 0.8 μm in diameter. It occurs with similar-sized bleb-like grains of chalcopyrite. The composition of the Pd antimonide (Table 2, grain 4) resembles mertieite I $[(Pd,Cu)_{5+}(Sb,As)_{2-}$ or $(Pd,Cu)_{11}(Sb,As)_4]$, mertieite II $[(Pd,Cu)_8(Sb,As)_3]$, and stibiopalladinite $[(Pd,Cu)_{5+}(Sb,As)_{2-}]$ (Cabri & Laflamme 1981). The composition also appears to be As-rich relative to mertieite II and stibiopalladinite in other rocks, and As-poor relative to mertieite I (Cabri & Laflamme 1981, Prichard & Tarkian 1988).

Pd–Ag sulfide

The single grain of Pd–Ag sulfide observed in the LM occurs within 50 μm of the Pd antimonide (Fig. 3F). The Pd–Ag sulfide grain measures 0.8 by 0.5 μm. It is at the margin of a rock fracture and is slightly elongate parallel to the fracture. This mineral is compositionally distinct from vysotskite (PdS), because it is Ag-rich, Ni-poor and metal-rich (M/S = 1.5) relative to natural vysotskite (Cabri & Laflamme 1981) and ideal PdS stoichiometry (Table 2, grain 5). Its composition apparently corresponds most closely to Pd_2AgS_2, and may represent a new mineral species.

Sperrylite

Sperrylite is present in both the LM and the UM. All of the grains are micrometric to submicrometric. They occur as bleb-shaped grains dispersed in a rectangular pattern about a grain of kotulskite within a chalcopyrite grain (Fig. 4A), in secondary silicate alteration (ferro-hornblende, titanite and chlorite) within altered Fe–Ti oxide (Fig. 4B), in pyrite (Fig. 4C), and in amphibole near small grains of chalcopyrite within altered groundmass. Sperrylite grains isolated in an area of secondary silicate alteration and in pyrite (cobaltian, 1.2 at.% Co) commonly have a thin rim of kotulskite. The largest grain of sperrylite in pyrite (Fig. 4C) is at a zonal boundary with As-bearing cobaltian pyrite (0.1 at.% As).

The ultrafine grain-size of sperrylite made *in situ* analysis difficult. Compositions of the sperrylite may have minor amounts of Pd (Table 2, grain 6) or S.

Rh–Pt sulfarsenide

The single grain of Rh–Pt sulfarsenide observed is in the UM, isolated in epidote, near the contact with titanite at the margin of a large, kotulskite-bearing pyrite grain (Fig. 4D). The Rh–Pt sulfarsenide grain is bleb-like and submicrometric in size. Compositionally, this mineral is distinct from hollingworthite (RhAsS) because it is metal poor (M/S = 0.4, Table 2, grain 7) relative to natural hollingworthite (Cabri & Laflamme 1981) and ideal RhAsS. Its composition apparently corresponds most closely to $(Rh,Pt)(As,S)_2$, and may represent a new mineral species.

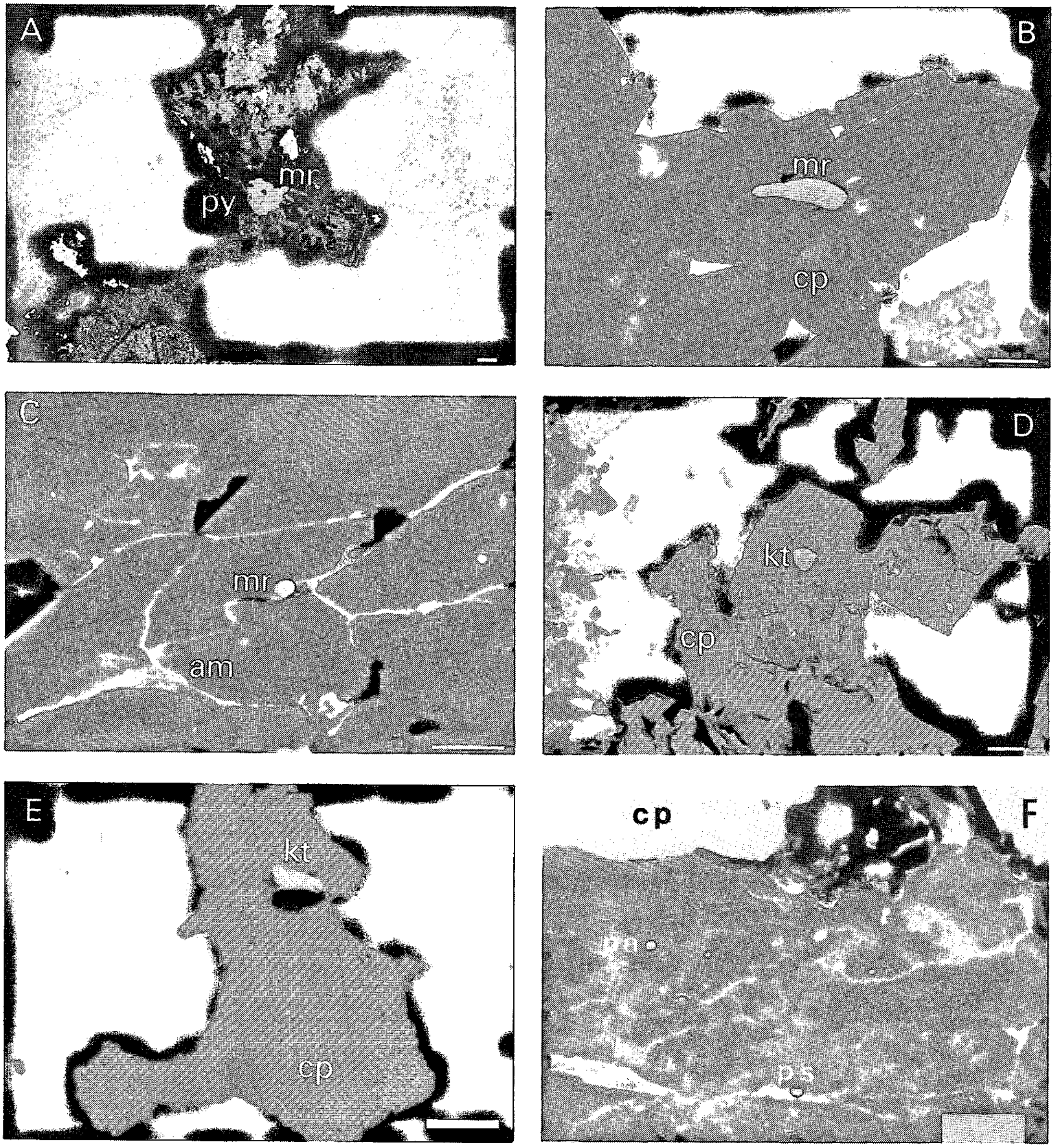

FIG. 3. Palladium minerals. A) Merenskyite (mr, bright) in pyrite (py) within the margin of altered Fe–Ti oxide (grey). B) Enlargement of A) showing association of merenskyite (mr, bright) with chalcopyrite (cp, pale grey) and fractures in pyrite. C) Merenskyite (mr) in amphibole (am) within the altered groundmass. D) Kotulskite (kt, bright) in chalcopyrite (cp, pale grey) within altered Fe–Ti oxide. E) Kotulskite (kt, bright) in contact with chalcopyrite (cp, pale grey) and an amphibole inclusion (dark), within altered Fe–Ti oxide. F) Pd antimonide (pa, bright) and Pd–Ag sulfide (ps, bright) in amphibolitized groundmass near large grain of chalcopyrite (cp, bright). A to E from the UM, F from the LM. Back-scattered electron images, except E (reflected light, crossed polars, oil). Scale bar: 10 μm in B, C, D, E and F, 100 μm in A.

TEXTURES AND SPATIAL ASSOCIATIONS

The primary mineralogy of the PGE-mineralized samples apparently consisted of cumulate clinopyroxene (70 modal %) and intercumulus Fe–Ti oxide (10 modal % in the spinel pyroxenite), and interstitial minor plagioclase, very minor apatite and possibly sulfides as well. During cooling

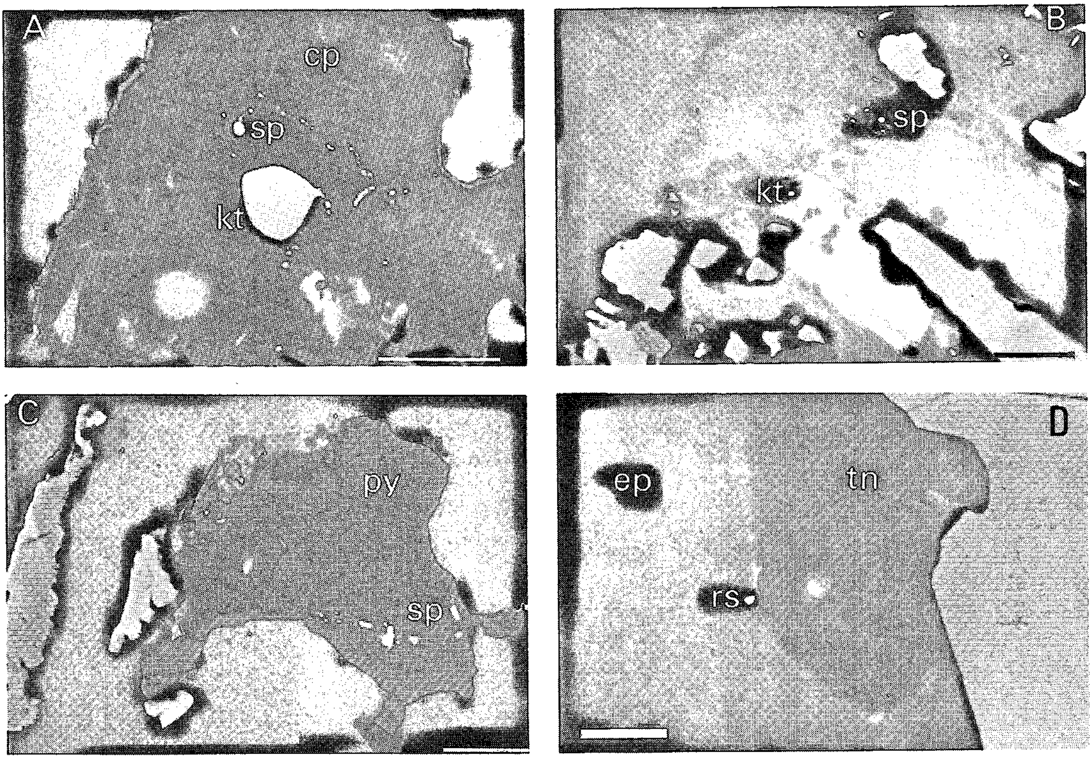

FIG. 4. Platinum minerals. A) Enlargement of 3D) showing sperrylite grains (sp, bright) dispersed about a kotulskite grain (kt, bright) in chalcopyrite (cp, grey) within altered Fe–Ti oxide. B) Grains of sperrylite (sp, bright) and kotulskite (kt, bright) in secondary silicate alteration of Fe–Ti oxide. C) Grains of sperrylite (sp, bright) in zoned cobaltian pyrite (py grey) within altered Fe–Ti oxide. D) Grain of Rh–Pt sulfarsenide (rs) in epidote (ep, dark grey) and titanite (tn, grey) at the margin of large grain of pyrite (py). From the UM. Back-scattered electron images. Scale bar: 10 μm.

of the flow and later greenschist-facies metamorphism, clinopyroxene and Fe–Ti oxide were altered to amphibole and titanite + amphibole + sulfide, respectively, plagioclase was altered to amphibole + albite + chlorite, and the groundmass was altered to amphibole + chlorite. However, relict clinopyroxene, diopside in composition, is preserved. Also, the Fe–Ti oxide shows a lamellar intergrowth of magnetite and ilmenite indicative of subsolidus exsolution at moderate temperatures (Stone *et al.* 1987). In the altered pyroxenite, which separates the LM and UM (Fig. 2), clinopyroxene and Fe–Ti oxide were more extensively altered. Despite this more extensive alteration, it is apparent that the proportion of Fe–Ti oxide progressively increased up-section in the pyroxenite layer approaching the contact with the spinel pyroxenite layer.

Bulk compositions of the LM and UM host samples in terms of the major and trace elements are given in Table 3. In the host sample of LM, the value given for Pt is semiquantitative because the correction for interference from Au was unduly large, reflecting the abnormally high content of Au in this sample. The PGE contents of the LM host rock are similar to those of pyroxenite samples of komatiitic and tholeiitic volcanic rocks from Munro Township (Crocket & MacRae 1986), but Au is abnormally high. However, the Pd and Pt contents of the UM host rock are higher than those of most pyroxenite samples from Munro Township.

The PGE mineralization in the BCF is further characterized by low contents of Cu, Ni and S (Table 4), and very minor proportions of sulfide minerals (<0.5 modal %), namely, chalcopyrite (70 modal %) and pyrite + bornite (30 modal %). Cobaltite, gersdorffite, linneite, sphalerite, and mackinawite are present, but rare. There is a virtual absence of nickel sulfide. The sulfides are commonly within or at the margins of altered Fe–Ti oxide grains (Figs. 3A, D, 4B), in close spatial association with secondary silicate alteration, and are therefore considered to be replacement of the oxide, specifically magnetite. A similar replacement of Fe

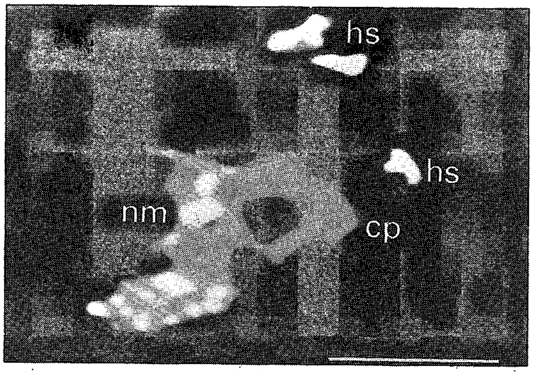

FIG. 5. Naumannite (nm, bright) and hessite (hs, bright) in spatial association with chalcopyrite (cp, grey) within grains of altered Fe–Ti oxide. From the LM. Back-scattered electron image. Scale bar: 10 μm.

oxide by sulfide has been reported for mineralization in the Duluth Complex (Pasteris 1984).

Compared to PGM grains observed in the UM, those in the LM are less abundant, finer grained and are located only in the altered groundmass. These PGM are associated with native gold, electrum, naumannite, an unnamed Ag–Bi selenide, hessite, and native silver, although not in very close proximity to them. The latter minerals are present as bleb-like micrometric to submicrometric grains. Native gold occurs in association with secondary silicates and calcite, and is pure gold in composition. Electrum is in a lamellar intergrowth with host hessite. Naumannite, unnamed Ag–Bi selenide, hessite and native silver occur in association with chalcopyrite and bornite grains within altered Fe–Ti oxide (Fig. 5). Compositions of the gold and silver minerals are given in Table 4. The single grain of unnamed Ag–Bi selenide is the only Bi-bearing grain observed in the LM. One grain of native gold was observed in the UM.

The PGM grains in the UM occur in sulfide and silicate alteration of oxide and in the altered groundmass. The Pd mineral grains, except merenskyite, that occur in fractures within pyrite are multifaceted (*e.g.*, Fig. 3B). The boundaries of one kotulskite grain in contact with chalcopyrite and actinolite in an inclusion (Fig. 3E) are straight against the former and slightly embayed and irregularly sutured against the latter. Grain boundaries of merenskyite, sperrylite, and Rh–Pt sulfarsenide are rounded in contact with secondary silicates.

Grains of sperrylite and Pd minerals are commonly in spatial association. Discrete grains of sperrylite and kotulskite occur in close proximity to each other in chalcopyrite and silicate alteration (Figs. 4A, B). Grains of sperrylite in silicate alteration and pyrite are commonly enclosed by a thin, irregular rim of kotulskite. One such sperrylite in a cleavage plane of the immediate amphibole host is slightly elongate parallel to the cleavage trace (Fig. 4B). Seven grains of sperrylite were observed dispersed in secondary silicate within 30 μm of a grain of sulfide-associated merenskyite.

DISCUSSION

The mineralogy, textures, and spatial associations of the PGM grains indicate an important role for secondary processes in the origin of the PGE mineralization in the Boston Creek Flow. The merenskyite, kotulskite, and chalcopyrite that occur in fractures in pyrite and the Pd–Ag sulfide in the rock fracture represent metal mobilization and reconcentration by hydrothermal fluids during cooling of the flow or later greenschist-facies metamorphism. Palladium, Te, Bi, Ag, Cu and S, as well as Pt and As, may be mobilized at moderate to low temperatures by hydrothermal fluids (Mountain & Wood 1988, McKibben *et al.* 1990, Nyman *et al.* 1990, Sassani & Shock 1990), and pyrite deforms by brittle failure under amphibolite- and greenschist-facies conditions (Gill 1969, Barrett *et al.* 1977). Hydrothermal processes have been proposed for PGE ± Cu–Fe sulfide mineralization at New Rambler in Wyoming (McCallum *et al.* 1976), Rathbun Lake in Ontario (Rowell & Edgar 1986), and Donaldson West and Blue Lake in Quebec (Dillon-Leitch *et al.* 1986, Beaudoin *et al.* 1990), and in the upper zone of the eastern Bushveld Complex (Harney & Merkle 1990).

The occurrence of PGM in the BCF as grains isolated in secondary silicates is consistent with PGE mineralization by hydrothermal processes. PGM grains formed from sulfide liquid are expected to be hosted by magmatic sulfides because the PGE partition preferentially into sulfide liquid (Stone *et al.* 1990). The association of PGM grains with secondary silicates in the Blue Lake deposit (Beaudoin *et al.* 1990), Donaldson West deposit (Dillon-Leitch *et al.* 1986), Troodos ophiolite (Prichard & Lord 1990), and upper zone of the eastern Bushveld Complex (Harney & Merkle 1990) has been cited as evidence for hydrothermal mineralization.

In addition, the anhedral, sutured and elongate shapes of the PGM grains at grain boundaries in contact with secondary silicates may result from limited mobilization of the PGE during growth of the silicates. This suggestion is supported by the similar shape of Cu–Fe sulfides isolated in and present at the margins of secondary silicates. Sutured contacts of PGM grains at grain boundaries with silicates in mineralized samples from the Munni Complex, Australia, have been attributed to mobilization of PGE during alteration of sulfide (Hoatson & Keays 1989). In the BCF, the evidence for PGE mobilization during growth of the silicates, together with the occurrence of PGM grains isolated in the silicates, alteration of the oxide, and presence of open and healed fractures in pyrite, imply a protracted history of metal mobilization and reconcentration.

The occurrence of Pd mainly as bismuthotellurides, and the presence of native gold, electrum, and Ag selenides and tellurides, support our hypothesis of hydrothermal mineralization. The presence of Pd bismuthotellurides in other PGE deposits, including the Messina copper mine in Transvaal (Mihálik *et al.* 1974), New Rambler (McCallum *et al.* 1976), and Rathbun Lake (Rowell & Edgar 1986), has been considered characteristic of hydrothermal processes. Gold enrichment is associated with hydrothermal PGE mineralization in ophiolites (Foose *et al.* 1985). Certainly, the restriction of the PGM grains in the BCF to just a few of the observed sulfide grains is consistent with formation by hydrothermal processes.

In addition, the presence of pyrite and sphalerite in the PGE mineralization, together with the virtual absence of Ni sulfide, further support our hypothesis of hydrothermal mineralization. Harney & Merkle (1990) regarded the common occurrence of pyrite and the presence of sphalerite in PGE mineralization in the upper zone of the eastern Bushveld Complex as evidence for hydrothermal processes. Sphalerite is unlikely to crystallize from sulfide liquid (MacLean & Shimazaki 1976). Nickel sulfide was anticipated in the PGE mineralization in the Boston Creek flow, given the Ni contents of the sample hosts, because a notable proportion of the sulfide fraction in other pyroxenite samples with similar Ni contents is nickeloan pyrrhotite and pyrite ± pentlandite. The paucity of nickel sulfide in the PGE mineralization may result from localized hydrothermal redistribution of both Ni and S. The possibility that the Ni is located in the silicate alteration, particularly amphibole and chlorite, or in the oxide phases, is to be investigated.

The spatial association of the LM and UM with the altered pyroxenite is consistent with PGE mineralization by hydrothermal processes. The degree of the alteration, mainly seen in the transformation of the igneous rock to amphibolite, is abnormally high here compared to that elsewhere within the cumulate layers of the flow. Therefore, the conditions ambient here during the alteration were distinct from those characteristic of greenschist-facies metamorphism. It is conceivable that Pd and Pt were mobilized and reconcentrated in adjacent, less-altered pyroxenite by hydrothermal fluids during the alteration. In the Troodos ophiolite, Pd and Pt may have been mobilized during hydrothermal alteration of gabbro and concentrated in fresher gabbro (Prichard & Lord 1990).

The PGE mineralization in the BCF is distinct from that hosted by komatiitic rocks in Australia (Hudson 1986) and Brazil (Marchetto 1990) because it is characterized by an association with Cu–Fe sulfides and pyroxenite, and an absence of nickel sulfide and Ir minerals (*e.g.*, irarsite). The Australian and Brazilian examples of PGE mineralization have been attributed to an origin by magmatic processes, with or without later reworking during regional metamorphism. Although the mineralization of the PGE in the BCF involved hydrothermal processes, whether the PGE were originally concentrated in the pyroxenite and spinel pyroxenite layers by magmatic processes (*e.g.*, Barnes & Naldrett 1987, Brügmann *et al.* 1987) or by hydrothermal fluids at high to moderate (*e.g.*, Johan *et al.* 1989, Stone & Fleet 1990) or low temperatures (*e.g.*, McCallum *et al.* 1976, Rowell & Edgar 1986) remains to be determined. Studies in progress will constrain the relative roles of low-temperature hydrothermal processes, high-temperature to late-magmatic processes, and primary igneous processes in the origin of the PGE mineralization. Regardless of any uncertainty about its origin, the presence of mineralization in the Boston Creek Flow demonstrates that PGE mineralization is possible in volcanic rocks of the Abitibi belt, even in the absence of nickel sulfide.

ACKNOWLEDGEMENTS

We thank R.L. Barnett for advice and expert assistance with operation of the electron microprobe. Critical reviews and comments by L.J. Cabri, J.H.G. Laflamme, an anonymous reviewer, and R.F. Martin were helpful. WES gratefully acknowledges a Natural Sciences and Engineering Research Council of Canada postdoctoral fellowship. The research was funded by Natural Sciences and Engineering Research Council of Canada through operating grants to MEF and JHC.

REFERENCES

ALAPIETI, T.T. & LAHTINEN, J.J. (1986): Stratigraphy, petrology, and platinum-group element mineralization of the early Proterozoic Penikat layered intrusion, northern Finland. *Econ. Geol.* **81**, 1126-1136.

AUGÉ, T. (1988): Platinum-group minerals in the Tiébaghi and Vourinos ophiolitic complexes: genetic implications. *Can. Mineral.* **26**, 177-192.

BARNES, S.-J. & NALDRETT, A.J. (1987): Fractionation of the platinum-group elements and gold in some komatiites of the Abitibi greenstone belt, northern Ontario. *Econ. Geol.* **82**, 165-183.

BARRETT, F.M., BINNS, R.A., GROVES, D.I., MARSTON, R.J. & MCQUEEN, K.G. (1977): Structural history and metamorphic modification of Archean volcanic-type nickel deposits, Yilgarn Block, Western Australia. *Econ. Geol.* **72**, 1195-1223.

BEAUDOIN, G., LAURENT, R. & OHNENSTETTER, D. (1990): First report of platinum-group minerals at Blue Lake, Labrador Trough, Quebec. *Can. Mineral.* **28**, 409-418.

BRENNER, T.L. (1990): The O'Toole nickel deposit, Morro do Ferro greenstone belt, Brazil. *Econ. Geol.* **85**, 904-920.

BRÜGMANN, G.E., ARNDT, N.T., HOFMANN, A.W. & TOBSCHALL, H.J. (1987): Noble metal abundances in komatiite suites from Alexo, Ontario, and Gorgona Island, Colombia. *Geochim. Cosmochim. Acta* **51**, 2159-2169.

CABRI, L.J. & LAFLAMME, J.H.G. (1981): Analysis of minerals containing platinum group elements. *In* Platinum-Group Elements: Mineralogy, Geology, Recovery (L.J. Cabri, ed.). *Can. Inst. Min. Metall., Spec. Vol.* **23**, 151-173.

CORFU, F., KROGH, T.E., KWOK, Y.Y. & JENSEN, L.S. (1989): U-Pb zircon geochronology in the southwestern Abitibi greenstone belt, Superior Province. *Can. J. Earth Sci.* **26**, 1747-1763.

CORRIVAUX, L. & LAFLAMME, J.H.G. (1990): Minéralogie des éléments du groupe du platine dans les chromitites de l'ophiolite de Thetford mines, Québec. *Can. Mineral.* **28**, 579-595.

CROCKET, J.H. & MACRAE, W.E. (1986): Platinum-group element distribution in komatiitic and tholeiitic volcanic rocks from Munro Township, Ontario. *Econ. Geol.* **81**, 1242-1251.

DILLON-LEITCH, H.C.H., WATKINSON, D.H. & COATS, C.J.A. (1986): Distribution of platinum-group elements in the Donaldson West deposit, Cape Smith Belt, Quebec. *Econ. Geol.* **81**, 1147-1158.

FOOSE, M.P., ECONOMOU, M. & PANAYIOTOU, A. (1985): Compositional and mineralogic constraints on the genesis of ophiolite hosted nickel mineralization in the Pevkos area, Limassol Forest, Cyprus. *Miner. Deposita* **20**, 234-240.

GARUTI, G. & RINALDI, R. (1986): Mineralogy of melonite-group and other tellurides from the Ivrea–Verbano basic complex, western Italian Alps. *Econ. Geol.* **81**, 1213-1217.

GILL, J.E. (1969): Experimental deformation and annealing of sulfides and interpretation of ore textures. *Econ. Geol.* **64**, 500-508.

HARNEY, D.M.W. & MERKLE, R.K.W. (1990): Pt–Pd minerals from the upper zone of the eastern Bushveld Complex, South Africa. *Can. Mineral.* **28**, 619-628.

HOATSON, D.M. & KEAYS, R.R. (1989): Formation of platiniferous sulfide horizons by crystal fractionation and magma mixing in the Munni layered intrusion, west Pilbara block, Western Australia. *Econ. Geol.* **84**, 1775-1804.

HUDSON, D.R. (1986): Platinum-group minerals from the Kambalda nickel deposits, Western Australia. *Econ. Geol.* **81**, 1218-1225.

JACKSON, S.L. & HARRAP, R.M. (1989): Geology of parts of Pacaud, Catharine, and southernmost Boston and McElroy Townships. *In* Summary of field work and other activities 1989. *Ontario Geol. Surv., Misc. Pap.* **146**, 125-131.

JENSEN, L.S. (1985): Stratigraphy and petrogenesis of Archean metavolcanic sequences, southwestern Abitibi Subprovince, Ontario. *In* Evolution of Archean Supracrustal Sequences (L.D. Ayres, P.C. Thurston, K.D. Card & W. Weber, eds.). *Geol. Assoc. Can., Spec. Pap.* **28**, 65-87.

JOHAN, Z., OHNENSTETTER, M., SLANSKY, E., BARRON, L.M. & SUPPEL, D. (1989): Platinum mineralization in the Alaskan-type intrusive complexes near Fifield, New South Wales, Australia. **1.** Platinum group minerals in clinopyroxenites of the Kelvin Grove prospect, Owendale Intrusion. *Mineral. Petrol.* **40**, 289-309.

JOLLY, W.T. (1980): Development and degradation of Archean lavas, Abitibi area, Canada, in light of major element geochemistry. *J. Petrol.* **21**, 323-363.

KINGSTON, G.A. & EL-DOSUKY, B.T. (1982): A contribution on the platinum-group mineralogy of the Merensky reef at the Rustenburg platinum mine. *Econ. Geol.* **77**, 1367-1384.

MACLEAN, W.H. & SHIMAZAKI, H. (1976): The partition of Co, Ni, Cu, and Zn between sulfide and silicate liquids. *Econ. Geol.* **71**, 1049-1057.

MARCHETTO, C.M.L. (1990): Platinum-group minerals in the O'Toole (Ni–Cu–Co) deposit, Brazil. *Econ. Geol.* **85**, 921-927.

MCCALLUM, M.E., LOUCKS, R.R., CARLSON, R.R., COOLEY, E.F. & DOERGE, T.A. (1976): Platinum metals associated with hydrothermal copper ores of the New Rambler mine, Medicine Bow Mountains, Wyoming. *Econ. Geol.* **71**, 1429-1450.

MCKIBBEN, M.A., WILLIAMS, A.E. & HALL, G.E.M.

(1990): Solubility and transport of platinum-group elements and Au in saline hydrothermal fluids: constraints from geothermal brine data. *Econ. Geol.* **85**, 1926-1934.

MIHÁLIK, P., JACOBSEN, J.B.E. & HIEMSTRA, S.A. (1974): Platinum- group minerals from a hydrothermal environment. *Econ. Geol.* **69**, 257-262.

MOSTERT, A.B., HOFMEYR, P.K. & POTGIETER, G.A. (1982): The platinum-group mineralogy of the Merensky Reef at the Impala platinum mines, Bophuthatswana. *Econ. Geol.* **77**, 1385-1394.

MOUNTAIN, B.W. & WOOD, S.A. (1988): Chemical controls on the solubility, transport, and deposition of platinum and palladium in hydrothermal solutions: a thermodynamic approach. *Econ. Geol.* **83**, 492-510.

NYMAN, M.W., SHEETS, R.W. & BODNAR, R.J. (1990): Fluid-inclusion evidence for the physical and chemical conditions associated with intermediate-temperature PGE mineralization at the New Rambler deposit, southeastern Wyoming. *Can. Mineral.* **28**, 629-638.

PASTERIS, J.D. (1984): Further interpretation of the Cu-Fe-Ni sulfide mineralization in the Duluth Complex, northeastern Minnesota. *Can. Mineral.* **22**, 39-53.

PRICHARD, H.M. & LORD, R.A. (1990): Platinum and palladium in the Troodos ophiolite complex, Cyprus. *Can. Mineral.* **28**, 607-618.

______ & TARKIAN, M. (1988): Platinum and palladium minerals from two PGE-rich localities in the Shetland ophiolite complex. *Can. Mineral.* **26**, 979-990.

ROWELL, R.F. & EDGAR, A.D. (1986): Platinum-group element mineralization in a hydrothermal Cu-Ni sulfide occurrences, Rathbun Lake, northeastern Ontario. *Econ. Geol.* **81**, 1272-1277.

SASSANI, D.C. & SHOCK, E.L. (1990): Speciation and solubility of palladium in aqueous magmatic-hydrothermal solutions. *Geology* **18**, 925-928.

STONE, W.E., CROCKET, J.H. & FLEET, M.E. (1990): Partitioning of palladium, iridium, platinum, and gold between sulfide liquid and basalt melt at 1200°C. *Geochim. Cosmochim. Acta* **54**, 2341-2344.

______ & FLEET, M.E. (1990): Platinum–iron alloy (Pt_3Fe) in kimberlite from Fayette County, Pennsylvania. *Am. Mineral.* **75**, 881-885.

______, JENSEN, L.S. & CHURCH, W.R. (1987): Petrography and geochemistry of an unusual Fe-rich basaltic komatiite from Boston Township, northeastern Ontario. *Can. J. Earth Sci.* **24**, 2537-2550.

WILSON, A.H. & TREDOUX, M. (1990): Lateral and vertical distribution of platinum-group elements and petrogenetic controls on the sulfide mineralization in the P1 pyroxenite layer of the Darwendale subchamber of the Great Dyke, Zimbabwe. *Econ. Geol.* **85**, 556-584.

Received January 8, 1991, revised manuscript accepted July 10, 1991.